Molecular Recognition and Atropisomerization of [5,10,15,20-Tetrakis(1-pentyl-3-pyridinio)porphyrinato]zinc(II) in Water

Tadashi Mizutani,* Takuya Horiguchi, Hiroshi Koyama, Ippei Uratani, and Hisanobu Ogoshi*

Department of Synthetic Chemistry and Biological Chemistry, Graduate School of Engineering, Kyoto University, Sakyo-ku, Kyoto 606-01

(Received July 23, 1997)

A cationic porphyrin host, [5,10,15,20-tetrakis(1-pentyl-3-pyridinio)porphyrinato]zinc(II), binds benzenecarboxylates, in water. The temperature dependence of the binding affinity showed that the binding was entropically driven: for the binding of 1,2,4,5-benzenetetracarboxylate, $\Delta H^\circ = 4.36$ kJ mol^{-1} and $\Delta S^\circ = 95.4$ J K^{-1} mol^{-1}. The atropisomerization rates of the porphyrin were investigated by ^{1}H NMR, and were decelerated by the addition of either anionic guests or simple inorganic salts. Electrostatic interactions and accompanying desolvation mainly controlled these equilibrium and kinetic behaviors.

Molecular recognition in water has been one of the main subjects of interest for decades. A number of studies using cyclodextrins and cyclophanes have revealed that van der Waals interactions and electrostatic interactions mainly control the molecular-recognition behavior in water.[1] It is also emphasized that attractive van der Waals interactions between host and guest are accompanied by the desolvation of water molecules from the interacting surface. This leads to the positive translational entropy of released water serving as one of the driving forces of complexation, namely the hydrophobic interaction. Compared to a number of efforts to elucidate the equilibrium of complexation, less attention has been paid to the kinetic aspects. The dynamics of complexation and conformational changes in water is fundamental for a number of biologically important processes, such as protein folding and allosteric control. With a simple model system, Cramer et al.[2] investigated the association and dissociation rates of cyclodextrin–aromatic guest complexes, showing that subtle changes in the structure sensitively affect the kinetics. As part of our program to elucidate the factors controlling the dynamics of molecular recognition,[3] we prepared water-soluble cationic porphyrins and studied their molecular-recognition behavior with particular emphasis on the dynamics of conformational changes.

Atropisomerization in *meso*-substituted porphyrins has been studied[4] owing to the important role of such functional porphyrins as catalysts and carriers. Several approaches have been made to control the rate of atropisomerization, such as photochemical control[4b,4c] and steric control. Sternhell et al.[4e] reported that the atropisomerization rate can be controlled by changing the *ortho* substituents on the *meso* phenyl groups based on the rate comparison for a series of tetraphenylporphyrins bearing H, F, Cl, Br, and I in the *ortho* positions, and ascribed the retardation to the steric effects. 5,10,15,20-Tetrakis(1-alkyl-2-pyridinio)porphyrin underwent slow isomerization, and each atropisomer has been separated and identified.[5] On the other hand, atropisomerization in the *meta* isomer, 5,10,15,20-tetrakis(1-alkyl-3-pyridinio)porphyrin, is much faster. We employed this cationic porphyrin as a host, and report here on the molecular-recognition behavior and its atropisomerization rates, which were sensitive to such externally controllable parameters as the anionic guest concentration and ionic strength.

Results

Cationic porphyrin **1** was prepared as receptors for an anionic guest in water. 5,10,15,20-Tetrakis(1-pentyl-3-pyridinio)porphyrin tetrachloride (**1·H$_2$·Cl$_4$**) was prepared by alkylating 5,10,15,20-tetra(3-pyridyl)porphyrin (Chart 1).[6] We expect that the pentyl groups on nitrogen could afford a hydrophobic binding pocket near to cationic sites above the porphyrin plane. **1·H$_2$·Cl$_4$** was characterized by ^{1}H NMR and elemental analysis.[7] Zinc was inserted in a usual procedure to yield **1·Zn·Cl$_4$**, which was identified by ^{1}H NMR

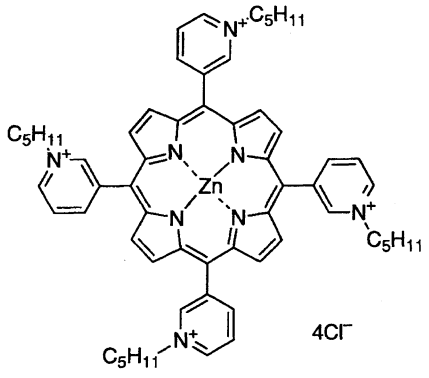

1•Zn•Cl$_4$

Chart 1.

and mass spectroscopy. In FAB mass, **1·Zn·Cl$_4$** did not give the parent signal, while in MALDI-TOF mass it gave the parent signal at $m/z = 1108$ ([M+H]$^+$, M = $C_{60}H_{68}N_8Cl_4Zn$) with its isotopomers. The isotopic distribution was in agreement with the calculated distribution, confirming its structure. **1·Zn·Cl$_4$** was soluble in polar solvents, such as water, methanol, and Me_2SO. The addition of chaotropic anions in a Hofmeister series, such as I^- and SCN^-, to an aqueous solution of **1·Zn·Cl$_4$** caused the precipitation of the porphyrin, while it was soluble in the presence of SO_4^{2-}, $H_2PO_4^-$, CH_3COO^-, and Cl^-. In water, the wavelengths of the absorption maxima of **1·Zn·Cl$_4$** remained constant at 430±1 and 558±1 nm over the concentration range of 1 μM to 1 mM, indicating that no aggregation occurred under our NMR conditions.[8)]

The ^{1}H NMR titration with **1·Zn·Cl$_4$** of a solution of tetrasodium 1,2,4,5-benzenetetracarboxylate (**4**) in D_2O showed that the aromatic C–H proton of the guest moved upfield by 0.9 ppm. Similarly, the aromatic protons of disodium terephthalate (**3**) and sodium benzoate (**2**) moved upfield by 2.1 and 0.6 ppm, respectively, displaying that **1·Zn·Cl$_4$** bound **2** and **3** (Chart 2). An analysis of the complexation-induced shifts as a function of the porphyrin concentrations gave the binding constants of these guests, which are listed in Table 1. The binding constant of **4** slightly increased along with increasing temperature over the range of 15—60 °C,[9)] showing that $\Delta H°$ was positive and that the binding was entropically driven. The binding constants of **3** decreased along with increasing temperature. In Table 2 are listed the values of $\Delta G°$, $\Delta H°$, and $\Delta S°$ obtained from a van't Hoff plot of the binding constants.

One of the unique features of these receptors is that the rate of atropisomerization was sensitive to the concentrations of both the anionic guests and inorganic ions. In the 500 MHz ^{1}H NMR of **1·Zn·Cl$_4$** in D_2O, the pyrrole β-protons appeared as a singlet above 5 °C. By adding anionic guests or inorganic ions, the β-protons appeared as a multiplet at low temperature, and coalesced at higher temperatures. Figure 1 shows the variable-temperature ^{1}H NMR of a solution of **1·Zn·Cl$_4$** and Na_2SO_4 in D_2O. The β-protons at 9.05 ppm coalesced at 45 °C. The coalescence temperature (T_c) is a measure of the rate of atropisomerization. Figure 2 shows the coalescence temperatures of the β-protons of **1·Zn·Cl$_4$** determined by 500 MHz ^{1}H NMR as a function of the ionic strengths of NaCl and Na_2SO_4 solutions, displaying that the addition of NaCl and Na_2SO_4 decelerated the isomerization rate. The chemical shift of the β-protons remained constant over the concentration range of NaCl from 0 to 0.25 M (1 M = 1 mol dm^{-3}) (I = 0—0.25 mol kg^{-1}), showing that no

Table 1. The Binding Constants of Anionic Guests by Cationic Zinc Porphyrin Host **1·Zn·Cl$_4$** in D_2O at 15 °C, and ^{1}H NMR Chemical Shifts of Free and Complexed Anionic Guests

Guest	K_a/M^{-1}	δ/ppm (free)	δ/ppm (complex)[b)]
4	16000±2200	7.51	6.57±0.01
3	5100±500	7.88	5.74±0.05
2	700±100	7.88[a]	7.31±0.06[a)]

a) The chemical shift of the lower field ortho proton was monitored. b) Calculated by the least-squares curve fitting.

Table 2. Thermodynamic Parameters for Complex Formation between **1·Zn·Cl$_4$** and Anionic Guests

Guest	$\Delta G_{288}°$/kJ mol^{-1}	$\Delta H°$/kJ mol^{-1}	$\Delta S°$/J K^{-1} mol^{-1}
4	−23.2	4.36	95.4
3	−20.4	−7.09	46.1

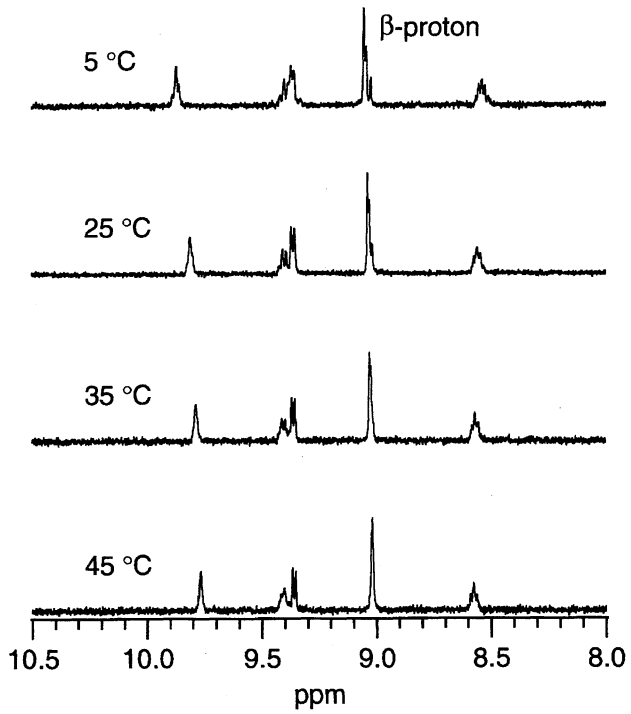

Fig. 1. Variable-temperature 500 MHz ^{1}H NMR of a solution of **1·Zn·Cl$_4$** and Na_2SO_4 in D_2O. [**1·Zn·Cl$_4$**] = 0.546 mM, [Na_2SO_4] = 0.162 M.

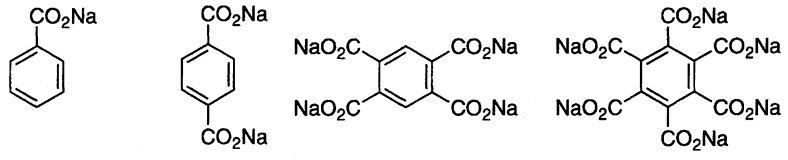

2 **3** **4** **5**

Chart 2.

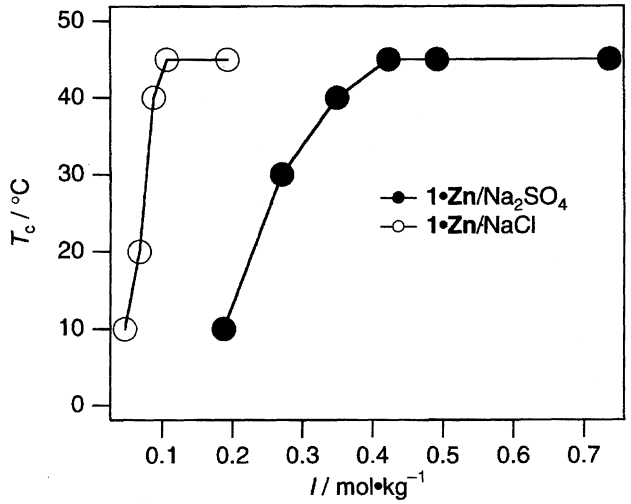

Fig. 2. Plot of the coalescence temperature (T_c) for the β-protons of **1** against ionic strength. Ionic strength was adjusted by either NaCl or Na_2SO_4. [**1·Zn·Cl$_4$**]=4.2×10^{-4} M for NaCl and 6.5×10^{-4} M for Na_2SO_4 in D_2O, 500 MHz ^{1}H NMR.

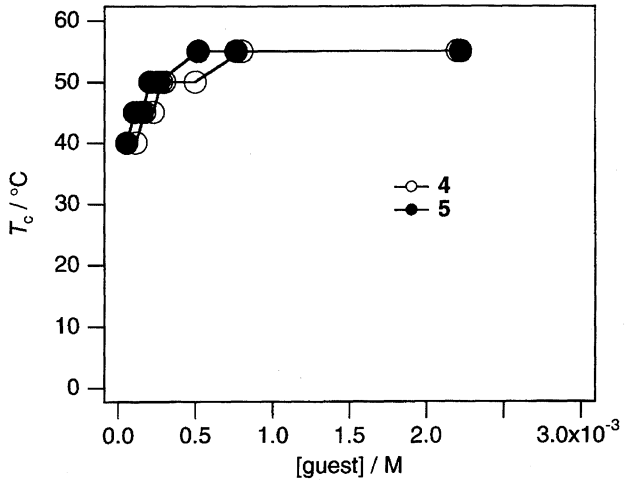

Fig. 3. Plot of the coalescence temperature (T_c) for the β-protons of **1** against guest concentrations. [**1·Zn·Cl$_4$**] = 5.7×10^{-4} M for **4** and 5.5×10^{-4} M for **5** in D_2O, 500 MHz ^{1}H NMR.

aggregation was induced by the addition of NaCl. In D_2O in the absence of inorganic ions, T_c was below 5 °C, while upon the addition of 0.14 M (I=0.14 mol kg^{-1}) of NaCl, T_c was raised to 45 °C. The coalescence temperatures were also determined by 270 MHz ^{1}H NMR, giving a lower coalescence temperature than that determined by 500 MHz NMR: T_c was 25 °C when the Na_2SO_4 concentration was 160 mM (I=0.48 mol kg^{-1}); the corresponding value of T_c determined by 500 MHz was 45 °C. These results established that the observed spectral changes originated from the kinetic process rather than the shifts in equilibrium.

The atropisomerization rate was decelerated as anionic guests were added. Figure 3 shows a plot of the coalescence temperature against the concentrations of **4** and **5**. The atropisomerization rate was decelerated as **4** and **5** were added. The coalescence temperature increased rapidly until one equivalent of **4** was added. In the presence of 0.1 equivalent of **5**, T_c was below 5 °C, while at 0.2 equivalent, T_c was 40 °C. Similarly, in the presence of 0.1—0.2 equivalent of **4**, T_c was below 5 °C, while at 0.3 equivalent of **4**, T_c was 40 °C. At the **4** concentration of 1 equiv or higher, the coalescence temperature was constant at 55 °C.

The addition of sodium acetate (0—0.16 M), NaH_2PO_4 (0—0.22 M), and imidazole (0—3.3 mM) did not cause the decoalescence of the β-protons of **1·Zn·Cl$_4$**. Thus, these ions did not decelerate the atropisomerization rate.

Table 3 summarizes the coalescence temperatures of **1·Zn·Cl$_4$** in the presence of amino acids. The addition of phenylalanine at pD 7.4 did not cause the decoalescence of the β-protons of **1·Zn·Cl$_4$**, even at 5 °C, while at pD 10.4, the coalescence temperature was raised to 15 °C. The addition of tyrosine at pD 10.4 also had retardation effects, with the coalescence temperature being raised to 40 °C.

Table 3. Effects of Amino Acids on the Coalescence Temperatures (T_c) of the β-Protons of **1·Zn·Cl$_4$** at pD 10.9[a)]

Amino acids	Concentration of amino acids/mM	T_c/°C
Phe	0.3	—
	0.6	15
	0.8	15
	2.4	15
Tyr	0.3	—
	0.5	35
	0.8	35
	1.0	35
	2.3	40

a) [**1·Zn·Cl$_4$**] = 5.9×10^{-4} M.

Discussion

Thermodynamics of Host–Guest Complexation: Molecular recognition by water-soluble cationic porphyrins was reported by Gaudemer[10)] and Kano.[11)] The importance of electrostatic interactions, either as a salt bridge or as microscopic charge polarization, was pointed out in these studies. The binding affinity of an ionic guest by an ionic host has been studied by Schneider et al.,[12)] who found that one salt bridge contributes 5 kJ mol^{-1} to the overall free-energy change in the complexation in water. Inoue et al.[13)] summarized the enthalpy change and entropy change of binding for a variety of host–guest complexes, their compilation revealing that, in most host–guest complexes, the complex formation was enthalpically driven (i.e., $\Delta H^\circ < 0$) with only a few exceptions. One such exception was reported by Shinkai et al.[14)] for complex formation between an anionic host and a cationic guest in water, where the enthalpy change in complexation was nearly zero and the entropy change was positive. In our system, the binding constants of **4** increased with increasing temperature over the range of 15 to 60 °C,[9)] indicating that the binding was entropically driven. We suppose

that two types of interactions, electrostatic interaction and hydrophobic interactions, are the major driving forces in this system. As shown in Table 2, the complex formation of **3** gave a negative enthalpy change, while that of **4** gave a positive enthalpy change; in both cases the entropy changes were positive. These observations suggest that water molecules are bound to the ionic groups of the host and guest, and that they are released to the bulk phase upon complexation. The positive translational entropy of released water molecules would lead to positive entropy changes for the overall thermodynamics of complexation, and the desolvation would lead to a positive enthalpy change. The negative enthalpy change associated with the electrostatic attractive forces between cationic sites of **4** and the anionic group of the guest would partly cancel the positive enthalpy change, owing to the desolvation; thus, the balance of these terms determines the sign of the overall enthalpy change.

Factors Controlling Atropisomerization: In the ortho isomers of **1·Zn·Cl$_4$**, the atropisomerization was slow and each atropisomer was separated and isolated.[5] However, since in **1·Zn·Cl$_4$**, the rate was much faster and comparable to the NMR time scale at room temperature, the isolation of each atropisomer was not attempted. Owing to this flexible nature, this host is suitable as a model to elucidate the major factors controlling the conformational dynamics in water.

Two major findings concerning the dynamics are that (1) the atropisomerization rate was decelerated by the addition of anionic guests or amino acids, and (2) it was also decelerated by the addition of simple inorganic salts. Because the effective concentrations of these additives greatly differ, we expect that different mechanisms are operating in these cases. One plausible explanation for the effects of the ionic strength is that the cationic charge of the pyridinium ring is localized in the initial state, while it is delocalized into the porphyrin ring due to the coplanar geometry. By increasing the ionic strength, this charge repulsion becomes negligible, stabilizing the initial state relative to the transition state, and decelerating the atropisomerization rate. This was checked by calculating the atomic charges by molecular-orbital calculations. The molecular-orbital calculation was performed for a model compound, [5-(1-methyl-3-pyridinio)porphyrinato]-zinc(II). The geometries of the ground state and the transition state optimized at the PM3 level are shown in Fig. 4, displaying that the pyridinium ring is perpendicular to the porphyrin plane in the initial state, while they are nearly coplanar in the transition state. The atomic charges calculated at the 3-21G* level for these geometries based on the orthogonal natural atomic orbitals[15] are listed in Table 4. The absolute values of the atomic charges are smaller in the transition state, except for C6, revealing that the transition state is less polar than the initial state.

As shown in Fig. 2, at 0.11 M (I=0.11 mol kg^{-1}) of NaCl and 0.14 M (I=0.42 mol kg^{-1}) of Na_2SO_4, the isomerization rate of **1·Zn·Cl$_4$** becomes constant. The screening lengths by the Debye–Hückel theory at these ionic strengths are 11.6 and 5.0 Å, respectively. These distances are comparable to the N–N distance between the two adjacent pyridine rings

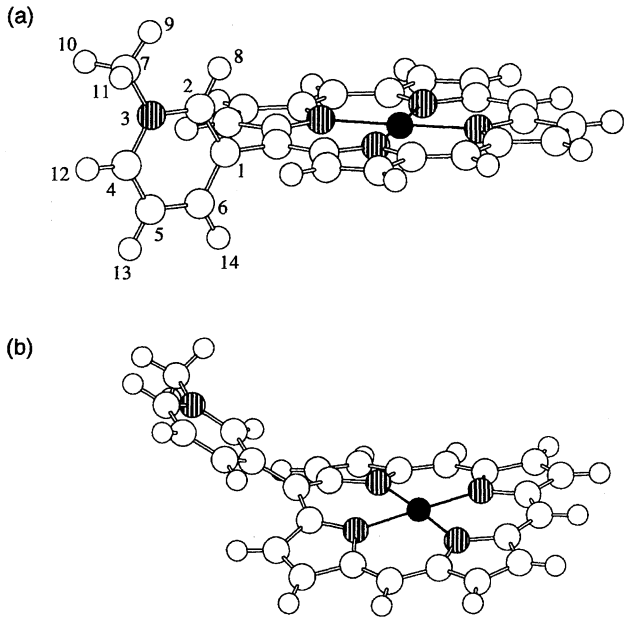

Fig. 4. The geometries of initial state (a) and the transition state (b) as calculated by semiempirical MO (PM3).

Table 4. Atomic Charges of a Model Porphyrin, [5-(1-Methyl-3-pyridinio)porphyrinato]zinc(II), in the Initial State and the Transition State[a]

	Initial state	Transition state
C1	−0.0698	−0.0438
C2	−0.7494	−0.7445
N3	−0.4090	−0.3889
C4	0.1091	0.0878
C5	−0.2972	−0.2871
C6	−0.0966	−0.1383
C7	−0.4428	−0.4401
H8	0.2922	0.2704
H9	0.2637	0.2610
H10	0.2641	0.2603
H11	0.2654	0.2642
H12	0.2824	0.2754
H13	0.2942	0.2879
H14	0.2988	0.2888
Zn	1.6731	1.6780

a) Based on orthogonal natural atomic orbitals at the 3-21G* level. For the atomic numbering scheme, see Fig. 4.

of **1·Zn·Cl$_4$**, 9—11 Å, as estimated by molecular modeling. Therefore, the concentration at which the coalescence temperature reaches a plateau corresponds to the distance at which the electrostatic repulsion between the two pyridine rings is unimportant, supporting our suggestion that neutralization of the cation–cation repulsion by added ions leads to slow atropisomerization.

The addition of anionic guests also affected the atropisomerization rate. The rate was decreased until one equivalent of **5** was added. This stoichiometry clearly indicated that the complex formation decelerated the isomerization rate, possibly due to the stabilization of the ground state relative to

the transition state. It is noteworthy that only 0.1 equivalent of **5** and 0.2 equivalent of **3** can cause a deceleration of the isomerization rate. This is apparently due to the faster association–dissociation than the isomerization, as shown in the ^{1}H NMR spectra, where only the averaged signals of the free and complexed species were observed. Thus, the anionic guest acts as a negative catalyst, decelerating the isomerization, with one molecule of the guest affecting the dynamics of 5 to 10 molecules of **1·Zn·Cl$_4$**.

Gaudemer et al.[10] reported that, in alkaline solutions, [5,10,15,20-tetrakis(1-methyl-4-pyridinio)porphyrinato]zinc(II) binds amino acids via a coordinating interaction between zinc and the amino group as well as the electrostatic interaction between the pyridinium cations and the carboxylate anions. In our system, a similar binding mode is expected for amino acids, which also decelerated the atropisomerization rate. The deceleration effects depended on the pD value of the media and the side-chain group of amino acids.

The addition of acetate, phosphate, and imidazole did not cause deceleration of isomerization, which cannot be readily explained. One can suggest that the coordination to zinc would stabilize the transition state, since MO calculations indicate that the positive charge on zinc in the transition state is larger than that in the initial state. However, this mechanism is not consistent with the deceleration observed for amino acids that also coordinate to zinc.

In summary, the cationic porphyrin was found to bind anionic guests with the entropic driving force. For the dynamic aspects, several factors are controlling the conformational changes in the cationic porphyrin in water. Intramolecular electrostatic forces are affected by the ionic strength of the media, controlling the dynamic features of the molecule. The addition of a guest also affected the dynamics in a more sensitive way than did the ionic strength, with only a catalytic amount of anionic guests exhibiting retardation. The addition of amino acids showed retardation effects, depending on the pD of the media and the structure of the side chain group of amino acids. Therefore, the coordination interaction between zinc and the amino group and the intermolecular interaction between the side-chain group of amino acid and the porphyrin influenced the dynamics of conformational changes in the cationic porphyrin.

Experimental

General. *N,N*-Dimethylformamide was distilled from CaH_2; 3-Pyridinecarbaldehyde, pyrrole, 1-iodopentane, methyl iodide were distilled just before use. ^{1}H NMR spectra were recorded on a JEOL A-500 spectrometer and a JEOL EX-270 spectrometer. FAB Mass spectra were measured with a JEOL JMS-SX102A, and MALDI-TOF mass spectra were measured with a JEOL JMS-Elite using α-cyano-4-hydroxycinnamic acid as a matrix. Molecular-orbital calculations were carried out by Spartan 3.1 on Silcon Graphics Indigo XS24. The equilibrium geometry and the transition geometry were calculated at the PM3 level; for these geometries were performed the 3-21G* level calculations to obtain electronic charges. The binding constants were determined by observing the chemical-shift displacements of the guest protons as a function of the porphyrin concentrations, and by analyzing them with a nonlinear least-squares curve-fitting program.

Preparation of 5,10,15,20-Tetra(3-pyridyl)porphyrin: 3-Pyridinecarbaldehyde (7 mL, 74.2 mmol) and pyrrole (5.1 mL, 73.5 mmol) were successively added to a mixture of propionic acid (260 mL) and acetic acid (4 mL) at room temperature. After being refluxed for 1.5 h, this solution was evaporated to dryness under a vacuum. A black tar-like product was dissolved in chloroform, and the organic layer was washed successively with water and dilute aqueous ammonia, and then evaporated in vacuo. The residue was purified by column chromatography on silica gel ($CHCl_3$: MeOH = 20 : 1) and recrystallized from MeOH to obtain 5,10,15,20-tetrakis-(3-pyridyl)porphyrin (1.61 g, 13.8%). ^{1}H NMR (500 MHz, $CDCl_3$) δ = 9.47 (s, 4H), 9.08 (dd, J = 1.7, 5.1 Hz, 4H), 8.87 (s, 8H, β-pyrrole), 8.54 (d, J = 5.5 Hz, 4H), 7.79 (t, J = 5.5 Hz, 4H), −2.82 (s, 2H); FAB MS m/z 619 ($M+H^+$).

Preparation of 5,10,15,20-Tetrakis(1-pentyl-3-pyridinio)-porphyrin Tetraiodide: To a solution of 5,10,15,20-tetra(3-pyridyl)porphyrin (197 mg, 0.32 mmol) in DMF (100 mL) was added 1-iodopentane (10 mL, 76.6 mmol) under N_2; the solution was then heated at 80 °C for 2.5 h. After the solvent was evaporated, the residue was washed with ether to remove excess 1-iodopentane. The residue was recrystallized from MeOH–EtOH (purple powder, yield 329.3 mg, 73.3%). ^{1}H NMR (500 MHz, CD_3OD) δ = 10.09 (t, 4H), 9.59 (d, 4H), 9.46 (d, H), 9.18 (br, 8H, β-pyrrole), 8.65 (t, 4H), 5.00 (t, 8H), 2.35 (m, 8H), 1.61 (m, 8H), 1.54 (m, 8H), 1.02 (t, J = 7.3 Hz, 12H). Anal. Calcd for $C_{60}H_{70}N_8I_4$: H, 4.96; C, 51.06; N, 7.94%. Found: H, 4.73; C, 51.18; N, 8.14%.

Preparation of 5,10,15,20-[Tetrakis(1-pentyl-3-pyridinio)-porphyrinato]zinc(II) Tetrachloride Salt: To a solution of 5,10,15,20-tetrakis(1-pentyl-3-pyridinio)porphyrin tetraiodide (61.2 mg, 43.4 μmol) in MeOH (15 mL) was added a saturated solution of zinc acetate in MeOH (20 mL). After stirring for 30 min, a solution of NH_4PF_6 in H_2O was added. A reddish-purple precipitate was filtered off and washed with a minimal volume of H_2O. The precipitate was then dissolved in a minimal volume of CH_3CN, and passed through an ion-exchange column (Dowex, 1-X2, 50-100 mesh, Cl-form) eluted with CH_3CN : H_2O = 1 : 1. The solvent was evaporated, and the residue was recrystallized from EtOH–hexane to obtain 35.6 mg (74.0%) of the salt. ^{1}H NMR (500 MHz, CD_3OD) δ = 10.00 (br s, 4H), 9.51 (d, 4H), 9.38 (d, 4H), 9.06 (s, 8H, β-pyrrole), 8.58 (t, 4H), 4.97 (t, J = 7.3 Hz, 8H), 2.33 (m, 8H), 1.58 (m, 8H), 1.52 (m, 8H), 1.00 (t, J = 7.3 Hz, 12H); MALDI-TOF Mass m/z 1108 ($M+H^+$).

This work was supported by a Grant-in Aid for Scientific Research from the Ministry of Education, Science, Sports and Culture.

References

1) J.-M. Lehn, "Supramolecular Chemistry, Concepts and Perspectives," VCH Publishers, Inc., New York (1995).

2) F. Cramer, W. Saenger, and H.-C. Spatz, *J. Am. Chem. Soc.*, **89**, 14 (1967).

3) T. Hayashi, T. Asai, H. Hokazono, and H. Ogoshi, *J. Am. Chem. Soc.*, **115**, 12210 (1993); Y. Kuroda, J. Lintuluoto, and H. Ogoshi, *Tetrahedron Lett.*, **35**, 3729 (1994); T. Mizutani, S. Yagi, A. Honmaru, and H. Ogoshi, *J. Am. Chem. Soc.*, **118**, 5318 (1996); T. Mizutani, T. Murakami, and H. Ogoshi, *Tetrahedron Lett.*, **37**, 5369 (1996).

4) a) K. Hatano, K. Anzai, T. Kubo, and S. Tamai, *Bull. Chem. Soc. Jpn.*, **54**, 3518 (1981); b) R. A. Freitag, J. A. Mercer-Smith,

and D. G. Whitten, *J. Am. Chem. Soc.*, **103**, 1226 (1981); c) R. A. Freitag and D. G. Whitten, *J. Phys. Chem.*, **87**, 3918 (1983); d) K. Hatano, K. Kawasaki, S. Munakata, and Y. Iitaka, *Bull. Chem. Soc. Jpn.*, **60**, 1985 (1987); e) M. J. Crossley, L. D. Field, A. J. Forster, M. M. Harding, and S. Sternhell, *J. Am. Chem. Soc.*, **109**, 341 (1987).

5) T. Kaufmann, B. Shamsai, R. S. Lu, R. Bau, and G. M. Miskelly, *Inorg. Chem.*, **34**, 5073 (1995).

6) R. G. Little, J. A. Anton, P. A. Loach, and J. A. Ibers, *J. Heterocycl. Chem.*, **12**, 343 (1975).

7) Similar compounds with different alkyl chain lengths have been reported: T. Elangovan and V. Krishnan, *Chem. Phys. Lett.*, **194**, 139 (1992).

8) It is reported that [tetrakis(1-methylpyridinio)porphyrinato]-zinc(II) showed no tendency to aggregate in water: R. F. Pasternack, L. Francesconi, D. Raff, and E. Spiro, *Inorg. Chem.*, **12**, 2606 (1973). In non-polar solvents such as dichloromethane, tetrakis (1-methyl-3-pyridinio)porphyrin aggregates (Ref. 7).

9) The binding constants and temperature, K_a/M^{-1} (T/ °C) **4**: 16000 (15), 16500(30), 18500 (45), 20300 (60); **3**: 5100 (15), 4100 (30), 3600 (45), 3400 (60).

10) C. Verchere-Beaur, E. Mikros, M. Perree-Fauvet, and A. Gaudemer, *J. Inorg. Biochem.*, **40**, 127 (1990).

11) K. Kano, N. Tanaka, H. Minamizono, and Y. Kawakita, *Chem. Lett.*, **1996**, 925.

12) a) H.-J. Schneider, R. Kramer, S. Simova, and U. Schneider, *J. Am. Chem. Soc.*, **110**, 6442 (1988); b) H.-J. Schneider, T. Shiestel, and P. Zimmermann, *J. Am. Chem. Soc.*, **114**, 7698 (1992).

13) Y. Inoue, T. Hakushi, Y. Liu, L. Tong, B. Shen, and D. Jin, *J. Am. Chem. Soc.*, **115**, 475 (1993); Y. Inoue, Y. Liu, L.-H. Tong, B.-J. Shen, and D.-S. Jin, *J. Am. Chem. Soc.*, **115**, 10637 (1993).

14) S. Shinkai, K. Araki, T. Matsuda, and O. Manabe, *Bull. Chem. Soc. Jpn.*, **62**, 3856 (1989).

15) P. O. Lowdin, *Phys. Rev.*, **97**, 1474 (1955); A. E. Reed, R. B. Weinstock, and F. Weinhold, *J. Chem. Phys.*, **83**, 735 (1985).